Superlattices and Microstructures 33 (2003) 339–346

Superlattices and Microstructures

www.elsevier.com/locate/jnlabr/yspmi

Electroluminescence from a current-emitting nanostructured silicon device

Christine Meyer, Heribert Lorenz, Khaled Karrai*

Center for NanoScience and Sektion Physik, Ludwig-Maximilians University, Geschwister-Scholl-Platz 1, 80539 Munich, Germany

Accepted 5 February 2004

Abstract

A three-dimensional silicon based nanodevice mainly consisting of two conductive silicon cantilevers was fabricated out of silicon-on-insulator material by electron beam lithography, reactive ion etching, and fluoride based wet chemical etching. One of the cantilevers is bent and sticks to the silicon substrate while the other one is freely suspended. We observed electroluminescence in the visible range when a voltage of any polarity is dropped across both levers. The measured spectra covered the range 400–950 nm peaking at about 650 nm. The current applied to the device could tune the intensity of the electroluminescence spectrum. Light powers ranging from 160 fW to some pW were measured at frequencies up to 17 kHz. The origin of the electroluminescence is discussed in comparison to porous silicon and spark-processed silicon.
© 2004 Elsevier Ltd. All rights reserved.

Keywords: Electroluminescence; Nanoscale device; Porous silicon; Spark-processed silicon

1. Introduction

The possibility of obtaining interband light emission from silicon despite its indirect bandgap is a very promising feature making it possible to manufacture optical and electronic devices integrated all in one chip. Porous silicon has been considered to be a good candidate for this application since its discovery in 1990 [1, 2]. Efficient visible room-temperature photoluminescence (PL) is emitted from this material. Electroluminescence (EL) was observed only a few years later [3, 4]. The luminescence properties of silicon structures obtained using alternative fabrication techniques were soon developed and

* Corresponding author. Fax: +49-89-2180-3182.

0749-6036/$ - see front matter © 2004 Elsevier Ltd. All rights reserved.
doi:10.1016/j.spmi.2004.02.008

compared with those of porous silicon helping to understand the physical origin of the optical emission [5]. In 1992 spark-processed silicon was introduced as a candidate for silicon-based PL [6] and in 1995 EL was demonstrated in such devices [7]. The fabrication of silicon nanowires in the form of silicon pillars lying on monocrystalline silicon to produce a large area silicon light-emitting device was reported by Nassiopoulos et al. [8]. Here we report on a single addressable nanostructured silicon device showing EL in the visible and near-infrared regime. The device fabrication is fully compatible with standard silicon processing technology. The EL turns out to be highly spatially localized and thus has the potential to be used as a sub-wavelength sized light source.

2. Device fabrication

The device discussed here was originally intended to be a nanotweezers device as made of a pair of freely suspended silicon nanocantilevers [9]. Each of the levers is 4 μm long, and has a width and thickness of about 250 and 100 nm, respectively. They have their free ends at a distance of about 200 nm from each other with an overlap of 1 μm (see Fig. 1(a)). The fabrication started with silicon-on-insulator (SOI) material with a highly arsenic-doped silicon top-layer. The cantilever structure was defined by electron beam lithography in polymethylmethacrylate (PMMA). This structure was then inverted by a lift-off technique to 1.5 nm NiCr and 50 nm Au layers deposited by thermal evaporation. Additionally, larger parts with overlap to the cantilever structure (leads) were defined in photoresist by optical lithography. The photoresist as well as the evaporated metal served as a mask for reactive ion etching in CF_4. The etching was performed at a pressure of about 6 mbar and a power of 100 W ensuring a complete etching through the top silicon layer. Afterwards, the Au and NiCr layers were removed in aqua regia and chromium etch, respectively. The residual photoresist was stripped in acetone and in oxygen plasma. After this procedure, contact pads of 1.5 nm NiCr and 150 nm Au were deposited in the outer areas of the structure to be able to contact the structure electrically. The sample was then etched in buffered hydrofluoric acid for 3.5 min to remove the 400 nm buried oxide layer beneath the nanocantilevers and dried in a critical point dryer using isopropanole and CO_2. The freely suspended nanocantilevers of 4 μm length fabricated by this method were then bonded and a voltage of about 20 V was applied across the cantilevers. We found out that during this procedure, one of the cantilevers bent down and stuck to the substrate irreversibly. This bending was a result of electrostatic forces. We explain the irreversible sticking of the cantilever to the substrate (in addition to van-der-Waals forces) by current-induced welding. A SEM image of the resulting device is shown in Fig. 1(c) and (d).

3. Measurements and results

We found out that when a bias voltage in the range of 10–20 V was applied across the cantilevers, light emission from the device was seen under an optical microscope with an objective of magnification 100 and a numerical aperture of 0.8 suggesting that the emission intensity in the visible range does not exceed the pW level. The luminescence started at a

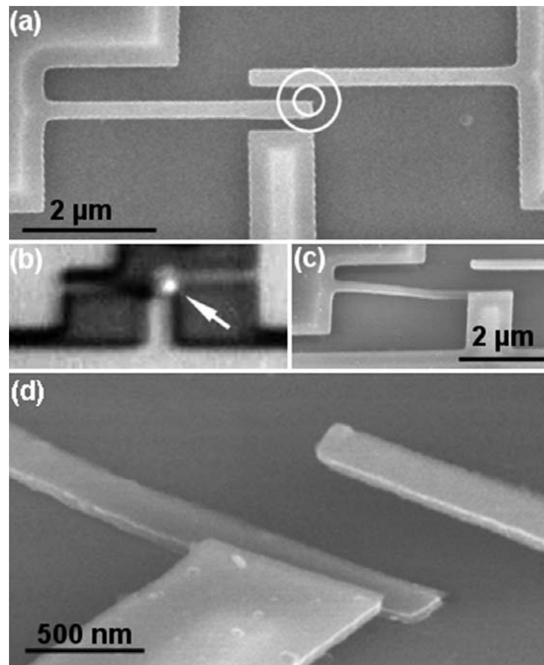

Fig. 1. SEM and optical microscope images. (a) SEM image of the sample before the voltage was applied that let one of the cantilevers stick to the substrate. Each of the two freely suspended cantilevers is 4 µm long. Two concentric rings mark the area where the light emission was observed. (b) Image of the light emitting device which was taken with a digital camera through an optical microscope with an objective of magnification 100 and a numerical aperture of 0.8. The arrow indicates the area where the light emission can be seen. The emitted light appears white to the eye. (c) SEM image of the sample after the voltage was applied. It is seen that the left cantilever is welded to the substrate. (d) Zoomed SEM image of the area showing clearly that one of the cantilevers is sticking to the substrate while the other one is still freely suspended.

distinct threshold voltage V_{th} and was restricted to a very small area at the end of the bent cantilever. Just before the emission became visible, a current in the range of some microamperes was measured. An image of the luminescent device taken with a digital camera through the microscope objective is shown in Fig. 1(b). The estimated position of the centre of the light emission is indicated in the scanning electron microscope (SEM) image in Fig. 1(a) by concentric rings. A schematic of the device is shown in Fig. 2 defining also the polarity of a positive bias (positive potential applied to the cantilever in contact with the Si substrate). A bending of the freely suspended cantilever towards the welded one or towards the substrate as a result of the applied voltage is likely to happen but it is estimated that it should not exceed a deflection of 20 nm. Therefore, the distance between the two cantilevers or between the free cantilever and the substrate of initially 400 nm is changed only slightly. This means that air as a barrier is always present at the voltages used. Therefore a tunnel current emission between silicon and air has to occur if a current is observed.

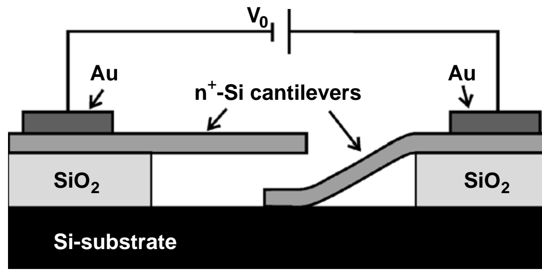

Fig. 2. Sample schematics. A schematic view of the sample is shown: one of the two free-standing cantilevers consisting of highly As doped silicon bent down to the lightly p-doped silicon substrate. Both cantilevers are contacted from outside using gold pads. The voltage is applied across the two cantilevers while the substrate is floating.

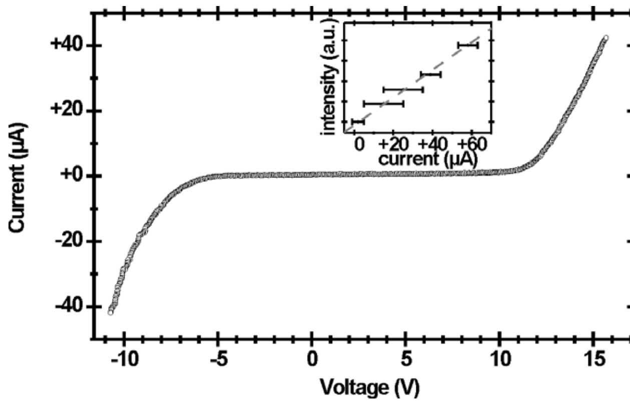

Fig. 3. I–V curve. A typical I–V curve of the device is shown. The curve was measured several times always showing a similar characteristic with the onset voltage varying from about 10 to 15 V for positive bias and from about −5 to −9 V for negative bias. The inset shows the luminescence intensity for positive bias to be roughly proportional to the current. The intensity was measured at constant voltages while the current drifted leading to relatively large error bars.

The I–V curve of the device is depicted in Fig. 3. Details of the measurement set-up are explained in footnote 1. It showed only very low current in the voltage range −5 to +11 V and a subsequent strong increase of the current up to 40 μA with increasing voltage up to +15 V. For negative bias the I–V-curve could be fitted exponentially, for positive bias an exponential fit was not possible. Since emission currents depend sensitively on the electric field and therefore on the distance between the cantilevers, a small deflection of the freely suspended cantilever could have a strong influence on the current voltage

[1] The I–V characteristic was measured using a 100 kΩ load resisitor in series with the sample in parallel with a voltage divider. The voltage divider consists of a 50 MΩ and a 20 MΩ resistor. The current and voltage at the sample were calculated from the voltage across the 20 MΩ resistor and the voltage applied to the whole system.

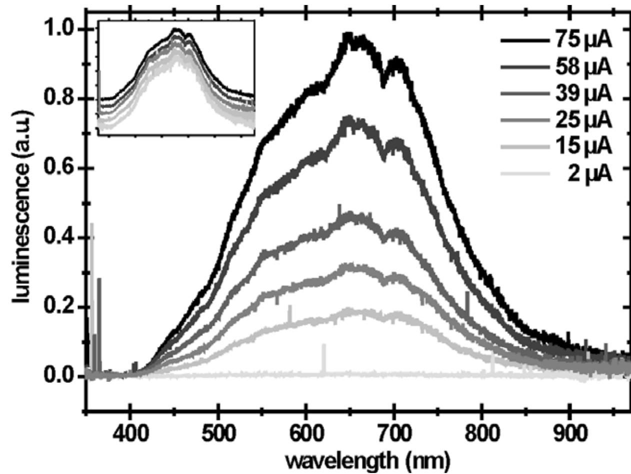

Fig. 4. Spectrum. The luminescence signal shown was measured at various currents with a CCD camera. All of the curves have a spectral range from about 400 to 950 nm. No shifts occur at higher currents (or voltages) and the substructure of the spectrum stays about the same. This can be seen very well from the inset showing all curves scaled to the same maximum and plotted with a small offset each.

characteristic despite of the change of only 20% in distance. The intensity of the emitted light was observed to be smaller at the same current for negative compared to positive bias. Currents at positive bias get larger if the device is illuminated with white light, presumably due to photon induced carrier generation, while this effect is not observed for negative bias. V_{th} did not have a fixed value but changed for different measurements in the range of 10–15 V. The EL still showed up after several months of sample storage at ambient conditions and with about the same characteristics suggesting a good robustness of the device.

The EL spectrum that is shown in Fig. 4 was measured using an objective (100×) with a numerical aperture of 0.8. The optical emission was dispersed in a 300 mm focal length grating spectrometer and detected with a nitrogen-cooled silicon CCD camera. The emission resulted in a broad-band spectrum distributed from 400 to 900 nm. The spectral range of the spectrometer set-up was 300–1050 nm. Measurements were performed for different voltages in the positively biased regime. The light intensities are roughly proportional to the emission currents as shown in the inset of Fig. 3. The spectra showed some substructures that hardly changed for different currents as depicted in the inset of Fig. 4. The spectral range also stayed constant and no spectral shift was detected.

The frequency response was measured using a dc voltage of 11 V (which was the threshold voltage for the following measurements) with a superimposed ac voltage with peak amplitudes varying from 1.4 to 4.2 V. This ensured that the emission was switched off completely once per cycle. The on/off switching of the light could be observed by eye through the objective up to a frequency of about 20 Hz. Using a Si PIN photodetector together with a current preamplifier (Stanford SR 570) feeding the input of a lock-in amplifier (Stanford SR 830), the electroluminesence was demodulated at the

switching frequency. A photo-signal was detected up to a frequency of 17 kHz. Higher frequencies could not be measured due to the cut-off of the current preamplifier at higher frequencies and for the high amplification gain used. The amplitudes of the signal measured were rather independent of the frequency applied and ranged from 160 fW to some pW.

4. Discussion

The EL of our device could have various origins. Since it first showed up after one of the cantilevers became welded to the substrate, changes in the cantilever are likely to have occurred during this process. A possible change is first of all a melting process. A voltage between the cantilever and the floating substrate induced the deflection of the cantilever towards the substrate. This would presumably have been accompanied by a discharge that has led to a quite high current density (which is very likely to occur due to the small size of the structure) and a subsequent change in the structure of the former single crystalline cantilever.

Many silicon-based light emitting devices have spectral signatures similar to the one we observed. When it comes to silicon-based EL, it is usual to think of porous silicon. This being said, however, the spectra observed there typically are smoother and show less substructure [4, 10] than the one measured here. The type of silicon EL having the most features in common with our device is spark-processed silicon [7, 11–13]. We speculate that the welding process resulted in a melted region in our device that resembles spark-processed silicon. During this process, the chemical constitution of the cantilever may have changed due to melting and oxidation effects. An alternative explanation for the electro-optical emission observed would be that the binding of the silicon cantilever to the silicon substrate led to some nanometer-sized silicon or silicon dioxide bridges enabling quantum size effects. One would then expect changes in the shape of the spectra with the voltage applied [5, 14] which were not observed here.

In order to obtain EL in the visible range in silicon, two conditions are mandatory: first, a radiative recombination or decay process enabling the luminescence and second, the presence of recombination or decay partners to actually luminesce. One mechanism proposed is the injection of electrons and holes into the luminescent region and a subsequent radiative recombination in quantized electronic states due to quantum size effects [4] or radiative recombination due to trapping in defect centres in the surrounding oxide [11]. Another possible mechanism is the tunnelling of hot electrons that leads to impact ionisation and the subsequent relaxation to the ground state via luminescing centres [12] or impurity scattering [15]. In both cases the shape of the interband optical emission spectra does not depend on the voltage in agreement with our observation. It should be noted that the origin of EL in spark-processed silicon is still not fully understood [13].

For the formation of spark-processed luminescent devices oxygen is required [11, 12]. It is reported that carrier recombination at luminescent centres in the oxide layer around Si nanoparticles may give the main contribution to EL [11]. EL is also observed from devices resembling spark-processed ones, but containing native oxide instead of the spark-processed region [16]. In similar samples, however, such EL was not observed [12]. Oxide compounds might have built in our device from the native oxide as well as during the melting process being performed at ambient conditions.

The EL spectrum of our device did not show any spectral shifts with voltage. Increasing voltages only led to an increasing EL intensity. This is also observed for devices consisting of lightly spark-processed silicon [11, 12], where a broad peak in the same spectral range with an analogous substructure is measured. A roughly linear dependence of the intensity on the current is observed for spark-processed silicon as well [11].

In general, the polarity dependence of non-crystalline silicon-based light emission is system dependent. For spark-processed silicon, for example, EL only appears for a specific polarity. This is, however, not the case for our device. As an explanation of the polarity dependence of EL in spark-processed silicon, it is proposed that hot electrons are injected into the spark-processed-Si by tunnelling and generate more electrons by impact ionisation. Some of these can then relax to the ground state via radiative pathways associated with defect states [12]. This could also explain the EL under one polarity for our device since there is a tunnelling barrier from the silicon to the air-filled gap leading to some hot electrons in the other cantilever. We observed a weaker EL for negative bias. This could be explained as a result of the lack of hot electrons in the active area. Here, EL might originate from electrons scattering at defects.

The different values of V_{th} we observed for different measurements can be explained by some structural changes, charging effects or surface modifications, e.g. desorption of water during the operation of the device. This may also be the reason for the current increase with time that was sometimes observed. A very similar behavior is known for silicon nanocrystal superlattices [17]. The different absolute values of V_{th} for positive and negative bias are presumably due to different local work functions leading to different emission probabilities at the two cantilevers.

In conclusion, we have introduced a new nanostructured silicon device exhibiting room-temperature EL in the visible range. Its properties are similar to those of spark-processed silicon except that a light emission was found for both electrical polarities. The fabrication is compatible with silicon process technology. In contrast to typical spark-processed devices, a potential barrier was created by an air-filled gap instead of a Schottky barrier at the metal contact. Hereby the active emission area is highly localized and is restricted to about a sub-wavelength size of 200 nm $\times$ 200 nm.

Acknowledgements

We would like to thank Alexander Högele for his help setting up the optical spectroscopy experiment and Armin Tilke for helpful discussions. The Deutsche Forschungsgemeinschaft (SFB 486 TPA2) is gratefully acknowledged for funding this project.

References

[1] L.T. Canham, Appl. Phys. Lett. 57 (1990) 1046.
[2] A.G. Cullis, L.T. Canham, P.D.J. Calcott, J. Appl. Phys. 82 (1997) 909.
[3] A. Richter, P. Steiner, F. Kozlowski, W. Lang, IEEE Electron Device Lett. 12 (1991) 691.
[4] N. Koshida, H. Koyama, Appl. Phys. Lett. 60 (1992) 347.
[5] See e.g. S. Tong, X. Liu, L. Wang, F. Yan, X. Bao, Appl. Phys. Lett. 69 (1996) 596; or W. Wu, X.F. Huang, K.J. Chen, J.B. Xu, X. Gao, J. Xu, W. Li, J. Vac. Sci. Technol. A 17 (1999) 159.

[6] R.E. Hummel, S.-S. Chang, Appl. Phys. Lett. 61 (1992) 1965.
[7] J. Yuan, D. Haneman, Appl. Phys. Lett. 67 (1995) 3328.
[8] A.G. Nassiopoulos, S. Grigoropoulos, D. Papadimitriou, Appl. Phys. Lett. 69 (1996) 2267.
[9] C. Meyer, H. Lorenz, K. Karrai, Appl. Phys. Lett. 83 (2003) 2420.
[10] B. Gelloz, T. Nakagawa, N. Koshida, Appl. Phys. Lett. 73 (1998) 2021.
[11] J. Yuan, D. Haneman, I. Andrienko, R. Siegele, P. Evans, Semicond. Sci. Technol. 13 (1998) 615.
[12] N. Shepherd, R.E. Hummel, J. Phys. Chem. Solids 64 (2003) 967.
[13] N. Shepherd, R.E. Hummel, Phys. Stat. Sol. (A) 197 (2003) 222.
[14] L.T. Canham, W.Y. Leong, M.I.J. Beale, T.I. Cox, L. Taylor, Appl. Phys. Lett. 61 (1992) 2563.
[15] C.W. Liu, S.T. Chang, W.T. Liu, M.-J. Chen, C.-F. Lin, Appl. Phys. Lett. 77 (2000) 4347.
[16] J. Yuan, D. Haneman, J. Appl. Phys. 86 (1999) 2358.
[17] V. Ioannou-Sougleridis, A.G. Nassiopoulou, T. Ouisse, F. Bassani, F.A. d'Avitaya, Appl. Phys. Lett. 79 (2001) 2076.